

Exotic mesons with hidden charm as diquark-antidiquark states

V.V. Anisovich⁺, M.A. Matveev⁺, A.V. Sarantsev^{+◇}, A.N. Semenova⁺

⁺*National Research Centre "Kurchatov Institute", Petersburg Nuclear Physics Institute, Gatchina, 188300, Russia*

[◇]*Helmholtz-Institut für Strahlen- und Kernphysik, Universität Bonn, Germany*

Abstract

Exotic mesons with hidden strange ($s\bar{s}$) and heavy quark pairs ($Q\bar{Q}$), where $Q = c, b$, are considered as diquark-antidiquark systems, $(Qs)(\bar{Q}\bar{s})$. Taking into account that these states can recombine into two-meson ones, we study the interplay of these states in terms of the dispersion relation D-function technique. The classification of exotic mesons is discussed, coefficients for decay modes are given, predictions for new states are presented. The nonet structure for $((Qq)(\bar{Q}\bar{q})$, $((Qs)(\bar{Q}\bar{s})$, $((Qq)(\bar{Q}\bar{s}))$ - states ($q = u, d$) is suggested.

PACS: 12.40.Yx, 12.39.-x, 14.40.Lb

1 Introduction

Presently we have several candidates for exotic mesons in the region of masses of charmonia $c\bar{c}$ and bottomonia $b\bar{b}$, see the PDG-compilation [1]. Some of them are debatable but on the whole the observations give a strong argument to the existence of such states. Here we discuss a scheme in which the exotic meson states are formed by standard QCD-motivated interactions (gluonic exchanges, confinement forces) but with diquarks as constituents. The formed diquark-antidiquark composite states should reveal themselves in decays caused by the recombination processes, see Fig. 1.

The construction of standard meson states with QCD-motivated interactions is a subject of multitudinous studies, without pretending for completeness we point out the refs. [2, 3, 4] and for the discussion of status of the meson states refs. [5, 6, 7] with references therein. The notion of the diquark was introduced by Gell-Mann [8]; for baryon states it is discussed for a long time, see pioneering papers [9, 10, 11, 12, 13] and conference presentations [14, 15, 16]. The systematization of baryons in terms of the quark-diquark states is presented in [17, 18]. The extension of the diquark notion to meson states leads to consideration of exotics, such extension in the sector of heavy diquarks is under discussion, see Maiani *et al.* [19], Voloshin [20], Ali *et al.* [21].

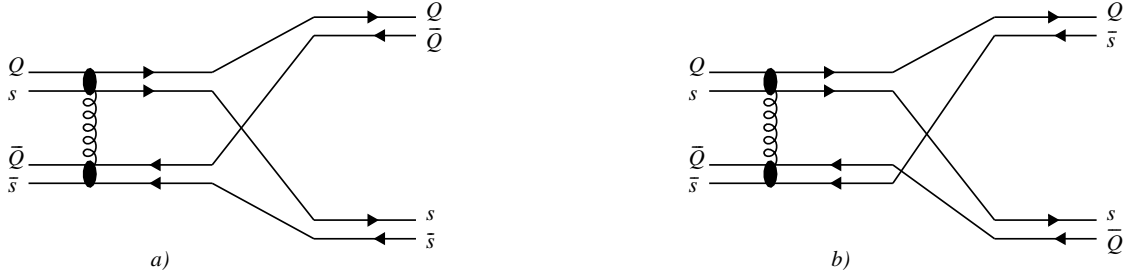


Figure 1: Exotic mesons as diquark-antidiquark states and their recombination into mesons.

In the paper we consider comparatively simple diquark-antidiquark systems, the exotic meson as a product of heavy-strange color diquarks:

$$(Qs) \cdot (\bar{Q}\bar{s}) = Q_{\alpha}s_{\beta} \varepsilon_{\alpha\beta\gamma} \varepsilon_{\alpha'\beta'\gamma} \bar{Q}_{\alpha'} \bar{s}_{\beta'}, \quad (1)$$

where indices $\alpha, \alpha', \beta, \beta', \gamma$ refer to color. Diquarks are supposed to be effective composite particles with constituent quarks in the S-wave that lead to two types of diquarks, scalar and axial-vector ones:

$$\begin{aligned} \text{scalar, } J^P = 0^+ & : (Qs)_{0^+} \equiv S_{(Qs)}, \\ \text{axial - vector, } J^P = 1^+ & : (Qs)_{1^+} \equiv A_{(Qs)}. \end{aligned} \quad (2)$$

Diquark-antidiquark states can recombine into two mesons:

$$\begin{aligned} \varepsilon_{\alpha\beta\gamma} \varepsilon_{\alpha'\beta'\gamma} &= \delta_{\alpha\alpha'} \delta_{\beta\beta'} - \delta_{\alpha\beta'} \delta_{\beta\alpha'}, \\ (Qs) \cdot (\bar{Q}\bar{s}) &= (Q\bar{Q})(s\bar{s}) - (Q\bar{s})(s\bar{Q}). \end{aligned} \quad (3)$$

Therefore, the exotic states are two-component systems with diquark-antidiquark and two-meson components. The dominance of the meson-meson component means that we deal with a molecule-like or deuteron-like system [22, 23, 24].

In this paper we consider tetraquark systems with hidden charm and hidden strangeness and study the interplay of the diquark-antidiquark and two-meson components in terms of dispersion relation D-function technique. A classification of these meson states is suggested and coefficients for decay modes are given. Comparison with existing data is discussed and predictions for new states are presented. The paper is organized as follows. In Section 2 we present a qualitative classification of the $(Qs) \cdot (\bar{Q}\bar{s})$ -systems following results of previous considerations [19, 20, 21] and a model treating $(Q\bar{Q})$ -systems [25, 26]. Spin and orbital momentum splittings of levels are given, the effect of strange quark weighting is estimated. The effect of recombination of diquark-antidiquark states into two-meson ones with subsequent meson-meson rescatterings play an important role in the formation of the singularities in the energy plane. We discuss the resulting singular structure of production amplitudes in Section 3 in terms of D-function technique for meson-meson channels. Comparison of calculations with data in the charmonium sector (Belle [27], CDF [28], CMS [29], D0 [30]) is given in Section 4. The determination of the mesons from the $(cs) \cdot (\bar{c}\bar{s})$ -sector allows to fix exotic mesons in non-strange sectors, $(cq) \cdot (\bar{c}\bar{q})$ where $q = u, d$, thus setting nonet classification for exotic mesons, Section 5.

The appendices are devoted to technicalities. In Appendix A we present the D-function method in terms of the dispersion relation technique for final state meson-meson rescatterings. Wave function decompositions for transitions of the diquark-antidiquark states into the meson-meson ones is given in Appendix B.

2 Classification of the diquark-antidiquark states

Here we present a qualitative classification of the $(Q_s) \cdot (\bar{Q}\bar{s})$ -systems, it is given in line with studies of [19, 20, 21] and model calculations of the $Q\bar{Q}$ -systems [25, 26]. We accept that diquarks and quarks, possessing similar color structure, allow similar model treating. Correspondingly, we guess that color forces result in similar mass splittings.

2.1 Low-lying states and diquark masses

Here we estimate masses of low-lying states keeping for a pattern results for $(Q\bar{Q})$ -systems which were obtained in [25, 26].

2.1.1 S-wave states

The lowest states are S-wave composite systems of diquark and antidiquark, they are as follows:

$$\begin{array}{l|l}
 J^{PC} & \Psi \\
 \hline
 2^{++} & \Psi_{ij}^{(AA)} = A_i^{(Qs)} \cdot A_j^{(Q\bar{s})} - \frac{1}{3}\delta_{ij} (A_\ell^{(Qs)} \cdot A_\ell^{(Q\bar{s})}) \\
 1^{+-} & \Psi_\ell^{(AA)} = \frac{1}{\sqrt{2}} \epsilon_{lij} (A_i^{(Qs)} \cdot A_j^{(Q\bar{s})}) \\
 0^{++} & \Psi^{(AA)} = \frac{1}{\sqrt{3}} (A_i^{(Qs)} \cdot A_i^{(Q\bar{s})}) \\
 1^{++} & \Psi_i^{[AS]} = \frac{1}{\sqrt{2}} (A_i^{(Qs)} \cdot S^{(Q\bar{s})} + S^{(Qs)} \cdot A_i^{(Q\bar{s})}) \\
 1^{+-} & \Psi_i^{\{AS\}} = \frac{1}{\sqrt{2}} (A_i^{(Qs)} \cdot S^{(Q\bar{s})} - S^{(Qs)} \cdot A_i^{(Q\bar{s})}) \\
 0^{++} & \Psi^{(SS)} = (S^{(Qs)} \cdot S^{(Q\bar{s})})
 \end{array} \tag{4}$$

where the indices (i, j, ℓ) refer to spin projections of the axial diquark.

Follow of the quark model estimations it is reasonable to consider diquark masses of the order of:

$$\begin{aligned}
 m_{(cq)} &\sim (1550 - 1850) \text{ MeV}, & m_{(cs)} &\sim (1650 - 1950) \text{ MeV}, \\
 m_{(bq)} &\sim (5050 - 5350) \text{ MeV}, & m_{(bs)} &\sim (5150 - 5450) \text{ MeV}.
 \end{aligned} \tag{5}$$

For comparison recall the masses of charmed and beauty quarks: $m_c \simeq 1275$ MeV [1], $m_c \simeq 1250$ MeV [25] and $m_b \simeq 4650$ MeV [1], $m_b \simeq 4500$ MeV [26], $4000 < m_b(QCD) < 4500$ MeV [31].

2.1.2 Mass splitting of states with different spins

Further we accept a simple mass formula which takes into account masses of constituents and spin splitting only:

$$m_{(q\bar{q})}^J = m_q + m_{\bar{q}} + J(J+1)\Delta. \tag{6}$$

Models for $(q\bar{q})$ -states tell us that $\Delta = (50 - 100)$ MeV.

2.2 Charmonium sector with hidden strangeness

We concentrate attention to states with hidden charm and strangeness, $(c\bar{c}s\bar{s})$, - these systems can be discussed on the basis of the observations of collaborations Belle [27], CDF [28], CMS [29], D0 [30] and LHCb [32].

2.2.1 Exotic states with hidden charm and strangeness, $(c\bar{c}s\bar{s})$

For charmed mesons (D, D^*, D_s, D_s^*) the weighting of the strange quark reads:

$$m_{D_s} - m_D \simeq m_{D_s^*} - m_{D^*} \simeq 100 \text{ MeV}. \quad (7)$$

We suppose the same value for the diquarks:

$$m_{(cs)} - m_{(cq)} \simeq 100 \text{ MeV}. \quad (8)$$

Further we restrict ourself by the consideration of the S-wave states. We do not include the state $X^{(1^{--})}(4660)$ into exotics because in this mass region there are two $(c\bar{c})$ states [25], namely, $\psi_{(5S)}(4570)$ and $\psi_{(4D)}(4710)$.

2.2.2 Suggested classification of the $cs \cdot \bar{c}\bar{s}$ -states

The following states with hidden strangeness are considered as diquark-antidiquark systems:

	observed peak	reaction, Γ, J^{PC}	classification
			$2^{++} \quad (A_{(Qs)} \cdot A_{(\bar{Q}\bar{s})})$ $\sim(4580 - 4680) \text{ MeV}$
			$1^{+-} \quad (A_{(Qs)} \cdot A_{(\bar{Q}\bar{s})})$ $\sim(4380 - 4420) \text{ MeV}$
Belle [27]:	$X_{(s\bar{s})}(4350 \pm 5)$,	$e^+e^- \rightarrow e^+e^-(\phi J/\psi)$, $\Gamma \simeq(5-30) \text{ MeV}, 0^{++}/2^{++}$	$0^{++} \quad (A_{(Qs)} \cdot A_{(\bar{Q}\bar{s})})$ $\sim 4280 \text{ MeV}$
CDF [28]:	$X_{(s\bar{s})}(4274 \pm 7)$,	$B \rightarrow K(\phi J/\psi)$, $\Gamma \simeq(20-50) \text{ MeV}, ?^{?+}$	$1^{++} \quad \frac{1}{\sqrt{2}}(A_s \cdot \bar{S}_s + S_s \cdot \bar{A}_s)$ $\sim(4310 - 4350) \text{ MeV} \quad (9)$
D0 [30]	$X_{(s\bar{s})}(4329 \pm 12)$	$\Gamma \simeq(12-62) \text{ MeV}, ?^{?+}$	
CMS [29]	$X_{(s\bar{s})}(4314 \pm 13)$	$\Gamma \simeq(8-88) \text{ MeV}, ?^{?+}$	
			$1^{+-} \quad \frac{1}{\sqrt{2}}(A_s \cdot \bar{S}_s - S_s \cdot \bar{A}_s)$ $\sim(4310 - 4350) \text{ MeV}$
		$B \rightarrow K(\phi J/\psi)$,	$0^{++} \quad (S_s \cdot S_s)$ $\sim 4140 \text{ MeV}$
CDF [28]:	$X_{(s\bar{s})}(4143 \pm 3)$,	$\Gamma \simeq(8 - 26) \text{ MeV}, ?^{?+}$	
D0 [30]	$X_{(s\bar{s})}(4159 \pm 11)$	$\Gamma \simeq(1-14) \text{ MeV}, ?^{?+}$	
CMS [29]	$X_{(s\bar{s})}(4148 \pm 9)$	$\Gamma \simeq(28 \pm 30) \text{ MeV}, ?^{?+}$	

Applying to the data [27, 28, 29, 30] the mass formula (6) we write mass parameters: $m_S = 2070 \text{ MeV}$, $m_A = 2140 \text{ MeV}$, $\Delta = (50 - 100) \text{ MeV}$. Value of the mass weighting for strange quark, see eq. (8), show to $X(3920)$ [1] as an analog of $X_{(s\bar{s})}(4148 \pm 9)$ in the $\omega J/\Psi$ system.

The $X_{(s\bar{s})}$ -states have a normal width, of the order $\Gamma \sim 30 \text{ MeV}$.

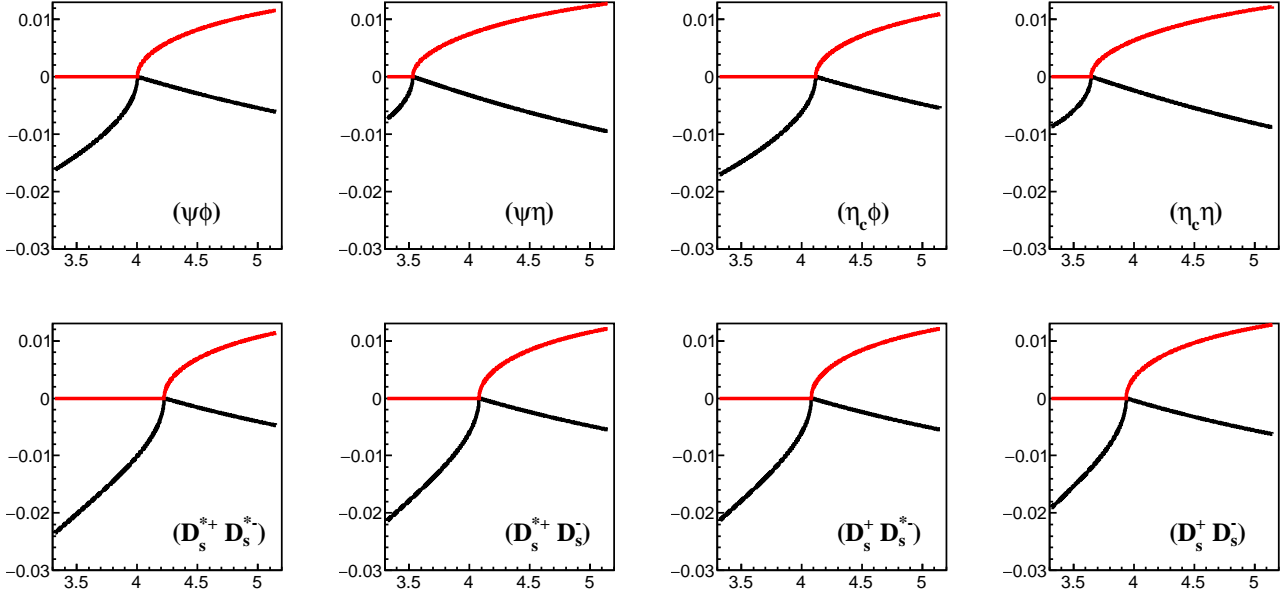


Figure 2: Imaginary (red) and real (black) parts of the loop diagrams $L_{\psi\phi}(s)$, $L_{\psi\eta}(s)$, $L_{\eta_c\phi}(s)$, $L_{\eta_c\eta}(s)$, $L_{D_s^{*+}D_s^{*-}}(s)$, $L_{D_s^{*+}D_s^-}(s)$, $L_{D_s^+D_s^{*-}}(s)$, $L_{D_s^+D_s^-}(s)$ at $g^2 = 1 \text{ GeV}^2$ as a functions of energy, \sqrt{s} . Thresholds are singular points.

3 Decomposition of the diquark-antidiquark states and meson-meson D-functions

It is reasonable to suggest that the recombination of quarks is responsible for the dominant mode of the decay, see Fig. 1. Using the dispersion relation D-function technique (see Appendix A and ref. [4] for more detail) we write resonance production amplitudes taking into account final state meson-meson rescatterings. Correspondingly, we present here loop diagrams for meson-meson transitions; necessary transformation of the diquark-antidiquark wave functions into meson-meson ones is given in Appendix B.

3.1 Loop diagrams for meson-meson rescatterings

Here for the production amplitudes of the studied diquark-antidiquark resonances (2^{++} , 1^{+-} , 0^{++} ; 1^{++} , 1^{+-} ; 0^{++}) we present decomposition of the spin wave functions into meson-meson ones and calculate corresponding meson-meson loop diagrams. In this way we write the D-functions which contain poles inherent to the resonances.

3.1.1 One-pole amplitude for the 2^{++} - state

Diquark-antidiquark classification gives one level for the S-wave 2^{++} - state that results in one-pole production amplitude. The spin wave function convolution (see Appendix B for detail) is

written for ($J_z = 0$) - state as follows:

$$\begin{aligned}
W_{(A_{(cs)}A_{(\bar{c}\bar{s})}) \cdot (A_{(cs)}A_{(\bar{c}\bar{s})})}^{(2^{++})} &= \left\langle \Psi_{(A_{(cs)}A_{(\bar{c}\bar{s})})}^{(2^{++}, J_z=0)} \mid \Psi_{(A_{(cs)}A_{(\bar{c}\bar{s})})}^{(2^{++}, J_z=0)} \right\rangle \\
&= \frac{2}{3} \langle \psi^{(0)} \phi^{(0)} \mid \psi^{(0)} \phi^{(0)} \rangle + \frac{1}{6} \langle \psi^{(\uparrow)} \phi^{(\downarrow)} \mid \psi^{(\uparrow)} \phi^{(\downarrow)} \rangle + \frac{1}{6} \langle \psi^{(\downarrow)} \phi^{(\uparrow)} \mid \psi^{(\downarrow)} \phi^{(\uparrow)} \rangle \\
&+ \frac{2}{3} \langle D_s^{*(+)(0)} D_s^{*(-)(0)} \mid D_s^{*(+)(0)} D_s^{*(-)(0)} \rangle + \frac{1}{6} \langle D_s^{*(+)(\uparrow)} D_s^{*(-)(\downarrow)} \mid D_s^{*(+)(\uparrow)} D_s^{*(-)(\downarrow)} \rangle \\
&+ \frac{1}{6} \langle D_s^{*(\downarrow)} D_s^{*(-)(\uparrow)} \mid D_s^{*(\downarrow)} D_s^{*(-)(\uparrow)} \rangle.
\end{aligned} \tag{10}$$

Loop diagrams $L_{2^{++}}$ (see Appendix A) are equal to:

$$L_{\psi\phi}(s) = \int_{(M_\psi+M_\phi)^2}^{+\infty} \frac{ds'}{\pi} \frac{\rho_{\psi\phi}(s')}{s' - s - i0}, \quad L_{D_s^{*+}D_s^{*-}}(s) = \int_{4M_{D_s^{*\pm}}^2}^{+\infty} \frac{ds'}{\pi} \frac{\rho_{D_s^{*+}D_s^{*-}}(s')}{s' - s - i0}, \tag{11}$$

where phase space factor reads

$$\rho_{\psi\phi}(s) = \frac{\sqrt{[s - (M_\psi + M_\phi)^2][s - (M_\psi - M_\phi)^2]}}{16\pi s} \Theta\left(s - (M_\psi + M_\phi)^2\right) \tag{12}$$

with $\Theta(x < 0) = 0$, $\Theta(x > 0) = 1$. For the $\rho_{D_s^{*+}D_s^{*-}}(s)$ one should replace in (12): $M_\psi \rightarrow M_{D_s^{*+}}$ and $M_\phi \rightarrow M_{D_s^{*-}}$.

The loop diagrams used in calculations are shown in Fig. 2, see also Appendix A. We keep $g^2 = \text{const}$ restoring the convergence of the dispersion relation integrals by the subtraction procedure.

Resonance production amplitude in D-function technique (for example, see [4]) reads:

$$A_{X \rightarrow \alpha}^{(2^{++})} = g_X \frac{1}{m_{2^{++}}^2 - s - g^2 \left[L_{\psi\phi}(s) + L_{D_s^{*+}D_s^{*-}}(s) \right]} g_\alpha, \quad \alpha = \psi\phi, D_s^{*+}D_s^{*-}, \tag{13}$$

where g_X, g_α refer to initial and final state couplings and $m_{2^{++}}$ is the input resonance mass which is roughly estimated in eq. (9): $m_{2^{++}} \simeq (4580 - 4680)$ MeV. Recall that the convergency of integrals with constant couplings g_X, g_α is ensured by subtraction procedure, see Appendix A for details.

Eq.(13) presents a generalization of the Breit-Wigner equation, graphically it is shown in Fig. 3 as an infinite set of the meson-meson loop diagrams.

The loop diagram $L_{D_s^{*+}D_s^{*-}}(s)$ reads:

$$\begin{aligned}
L_{D_s^{*+}D_s^{*-}}(s) &= \frac{1}{\pi} \sqrt{\frac{s - 4M_{D_s^{*\pm}}^2}{s}} \left[\frac{1}{\pi} \ln \frac{\sqrt{s} - \sqrt{s - 4M_{D_s^{*\pm}}^2}}{\sqrt{s} + \sqrt{s - 4M_{D_s^{*\pm}}^2}} + i \right], \quad s > 4M_{D_s^{*\pm}}^2 \\
L_{D_s^{*+}D_s^{*-}}(s) &= \frac{i}{\pi} \sqrt{\frac{-s + 4M_{D_s^{*\pm}}^2}{s}} \left[-\frac{2i}{\pi} \tan^{-1} \left(\frac{\sqrt{-s + 4M_{D_s^{*\pm}}^2}}{\sqrt{s}} \right) + i \right], \quad s < 4M_{D_s^{*\pm}}^2.
\end{aligned} \tag{14}$$

Subtraction is chosen to have $L_{D_s^{*+}D_s^{*-}}(s = 4M_{D_s^{*\pm}}^2) = 0$.

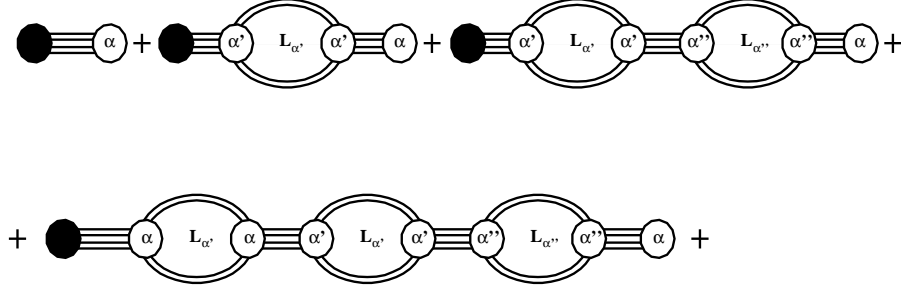


Figure 3: D-function pole amplitude as infinite set of diagrams with meson-meson rescatterings. For the 2^{++} state summing is performed over $\alpha, \alpha', \alpha'' = \psi\phi, D_s^{*+}D_s^{*-}$.

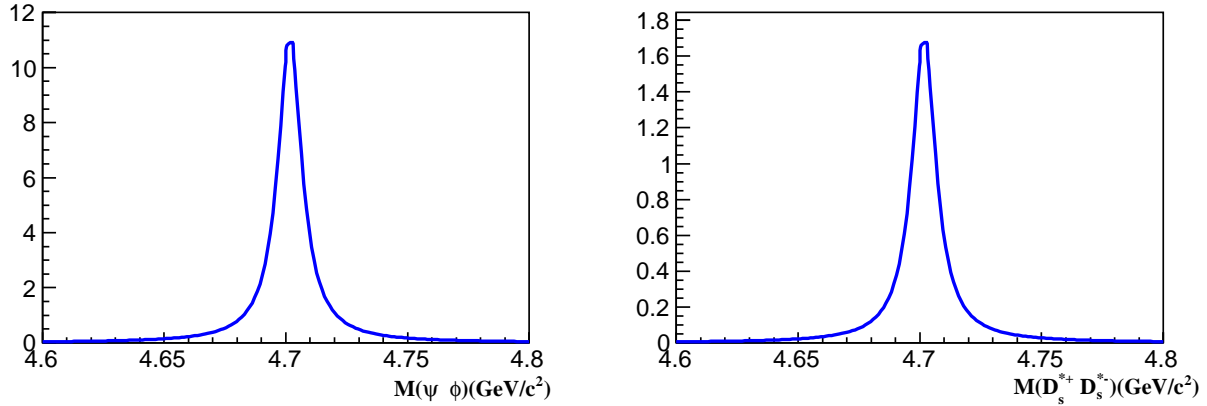


Figure 4: Production densities of the $\psi\phi$ and $D_s^{*+}D_s^{*-}$ states in the 2^{++} spectrum.

Separating real and imaginary parts of the amplitude, $A = \Re A + i\Im A$, we write for the particle production densities:

$$\begin{aligned}
 \sum_{S_z} \left| A_{X \rightarrow \psi\phi}^{(2^{++})} \right|^2 \rho_{\psi\phi} &= \frac{g_X^2 g_\alpha^2 \rho_{\psi\phi}}{\left[m_{2^{++}}^2 - s - g^2 \left(\Re L_{\psi\phi} + \Re L_{D_s^{*+}D_s^{*-}} \right) \right]^2 + \left[g^2 \left(\Im L_{\psi\phi} + \Im L_{D_s^{*+}D_s^{*-}} \right) \right]^2}, \\
 \sum_{S_z} \left| A_{X \rightarrow D_s^{*+}D_s^{*-}}^{(2^{++})} \right|^2 \rho_{D_s^{*+}D_s^{*-}} &= \frac{g_X^2 g_\alpha^2 \rho_{D_s^{*+}D_s^{*-}}}{\left[m_{2^{++}}^2 - s - g^2 \left(\Re L_{\psi\phi} + \Re L_{D_s^{*+}D_s^{*-}} \right) \right]^2 + \left[g^2 \left(\Im L_{\psi\phi} + \Im L_{D_s^{*+}D_s^{*-}} \right) \right]^2}, \quad (15)
 \end{aligned}$$

where summing is performed over meson spins at fixed J_z , see Eq. (10). Let us emphasize that the particle production densities are equal zero below the corresponding thresholds, namely, at $s < (M_\psi + M_\phi)^2$ for the $(\psi\phi)$ -channel and at $s < 4M_{D_s^{*\pm}}^2$ for the $(D_s^{*+}D_s^{*-})$ -channel. Production densities for the 2^{++} -state are shown in Fig. 4.

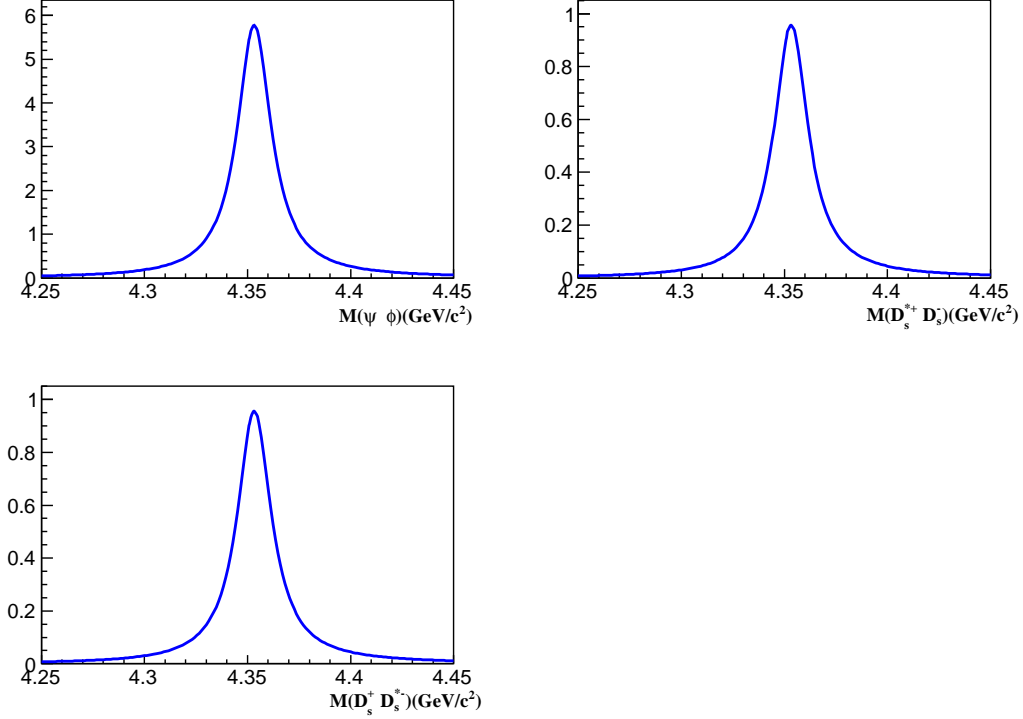


Figure 5: Production densities in $\psi\phi$ and $D^+D_s^{*-}$, $D^{*+}D^-$ spectra for the 1^{++} -states.

3.1.2 One-pole amplitude for the 1^{++} - state

For the ($J^{PC} = 1^{++}$, $J_z = 0$) - state the wave function convolution in meson space reads:

$$\begin{aligned}
 W_{[S_{(cs)}A_{(\bar{c}\bar{s})}]^{(1^{++})}} &= \frac{1}{2} \langle \psi^{(\uparrow)} \phi^{(\downarrow)} | \psi^{(\uparrow)} \phi^{(\downarrow)} \rangle + \frac{1}{2} \langle \psi^{(\downarrow)} \phi^{(\uparrow)} | \psi^{(\downarrow)} \phi^{(\uparrow)} \rangle \\
 &+ \frac{1}{2} \langle D_s^{*+(0)} D_s^- | D_s^{*+(0)} D_s^- \rangle + \frac{1}{2} \langle D_s^+ D_s^{*-(0)} | D_s^+ D_s^{*-(0)} \rangle,
 \end{aligned} \tag{16}$$

and the amplitude is written as:

$$\begin{aligned}
 A_{X \rightarrow \alpha}^{(1^{++})} &= g_X \frac{1}{m_{1^{++}}^2 - s - g^2 \left[L_{\psi\phi}(s) + \frac{1}{2} L_{D_s^{*+} D_s^-}(s) + \frac{1}{2} L_{D_s^+ D_s^{*-(0)}}(s) \right]} g_\alpha, \\
 \alpha &= \psi\phi, D_s^{*+} D_s^-, D_s^+ D_s^{*-(0)}.
 \end{aligned} \tag{17}$$

with bare mass given in eq. (9), $m_{1^{++}} \simeq (4310 - 4350)$ MeV.

Production densities for the 1^{++} - state are shown in Fig. 5.

3.1.3 Two-pole amplitude for the 1^{+-} - states

For the $J^{PC} = 1^{+-}$ we have two levels which can recombine into three meson-meson states. The wave functions for the ($J = 1$, $J_z = 0$) - states read:

$$\Psi_{(A_{(cs)}A_{(\bar{c}\bar{s})})}^{(1^{+-}, J_z=0)} = \frac{1}{\sqrt{2}} \left[\psi^{(0)} \eta + \eta_c \phi^{(0)} - D_s^{*+(0)} D_s^- - D_s^+ D_s^{*-(0)} \right], \tag{18}$$

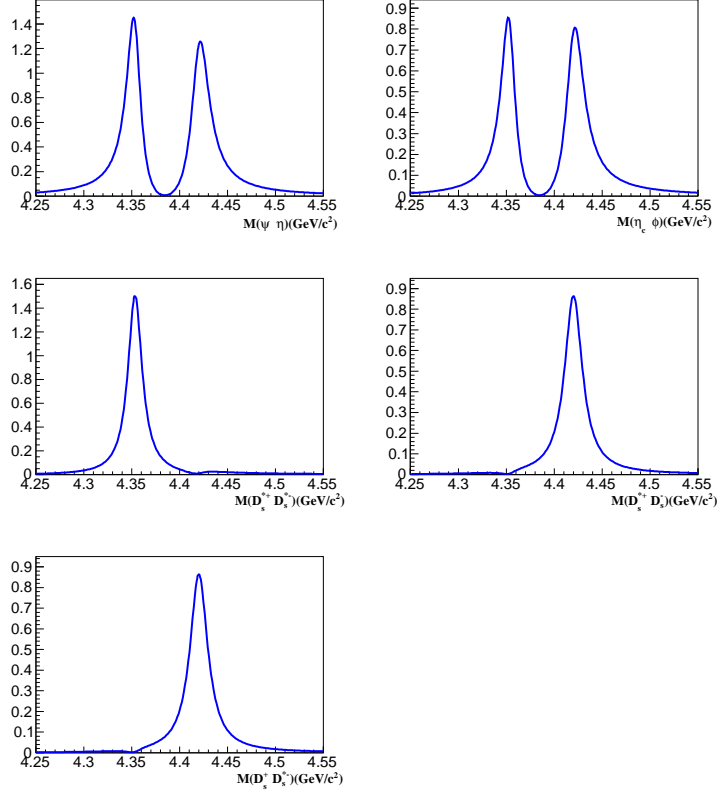


Figure 6: Production densities for the 1^{+-} - states. The red and green curves refer to case with switched-off mixing of different states.

$$\Psi_{\{S_{(cs)A(\bar{c}\bar{s})}\}}^{(1^{+-}, J_z=0)} = \frac{1}{\sqrt{2}} \left[-\psi^{(0)}\eta + \eta_c\phi^{(0)} - D_s^{*+(\uparrow)} D_s^{*-(\downarrow)} + D_s^{*+(\downarrow)} D_s^{*-(\uparrow)} \right].$$

Correspondingly we write the three meson-meson convolutions:

$$\begin{aligned} W_{(A_{(cs)A(\bar{c}\bar{s})})}^{(1^{+-})} &= \langle \Psi_{(A_{(cs)A(\bar{c}\bar{s})})}^{(1^{+-}, J_z=0)} | \Psi_{(A_{(cs)A(\bar{c}\bar{s})})}^{(1^{+-}, J_z=0)} \rangle = \frac{1}{2} \langle \psi^{(0)}\eta | \psi^{(0)}\eta \rangle \\ &+ \frac{1}{2} \langle \eta_c\phi^{(0)} | \eta_c\phi^{(0)} \rangle + \frac{1}{2} \langle D_s^{*+(0)} D_s^- | D_s^{*+(0)} D_s^- \rangle + \frac{1}{2} \langle D_s^+ D_s^{*- (0)} | D_s^+ D_s^{*- (0)} \rangle, \\ W_{(A_{(cs)A(\bar{c}\bar{s})}) \cdot \{S_{(cs)A(\bar{c}\bar{s})}\}}^{(1^{+-})} &= \langle \Psi_{(A_{(cs)A(\bar{c}\bar{s})})}^{(1^{+-}, J_z=0)} | \Psi_{\{S_{(cs)A(\bar{c}\bar{s})}\}}^{(1^{+-}, J_z=0)} \rangle \\ &= -\frac{1}{2} \langle \psi^{(0)}\eta | \psi^{(0)}\eta \rangle + \frac{1}{2} \langle \eta_c\phi^{(0)} | \eta_c\phi^{(0)} \rangle \\ W_{\{S_{(cs)A(\bar{c}\bar{s})}\}}^{(1^{+-})} &= \langle \Psi_{\{S_{(cs)A(\bar{c}\bar{s})}\}}^{(1^{+-}, J_z=0)} | \Psi_{\{S_{(cs)A(\bar{c}\bar{s})}\}}^{(1^{+-}, J_z=0)} \rangle = \frac{1}{2} \langle \psi^{(0)}\eta | \psi^{(0)}\eta \rangle + \frac{1}{2} \langle \eta_c\phi^{(0)} | \eta_c\phi^{(0)} \rangle \\ &+ \frac{1}{2} \langle D_s^{*+(\uparrow)} D_s^{*-(\downarrow)} | D_s^{*+(\uparrow)} D_s^{*-(\downarrow)} \rangle + \frac{1}{2} \langle D_s^{*+(\downarrow)} D_s^{*-(\uparrow)} | D_s^{*+(\downarrow)} D_s^{*-(\uparrow)} \rangle, \end{aligned} \quad (19)$$

and three loop diagram combinations:

$$\begin{aligned} L_{11}^{(1^{+-})} &= \frac{1}{2} g^2 L_{\eta_c\phi} + \frac{1}{2} g^2 L_{\psi\eta} + g^2 \frac{1}{2} L_{D_s^+ D_s^-} + g^2 \frac{1}{2} L_{D_s^+ D_s^{*-}}, \\ L_{12}^{(1^{+-})} &= -\frac{1}{2} g^2 L_{\psi\eta} + \frac{1}{2} g^2 L_{\eta_c\phi}, \end{aligned} \quad (20)$$

$$L_{22}^{(1+-)} = \frac{1}{2}g^2 L_{\eta_c\phi} + \frac{1}{2}g^2 L_{\psi\eta} + g^2 L_{D_s^{*+}D_s^{*-}}.$$

Indices 1, 2 refer to levels $1 \equiv \{A_{(Q_s)A_{(\bar{Q}\bar{s})}}\}$ and $2 \equiv \{S_{(Q_s)A_{(\bar{Q}\bar{s})}}\}$. The loop diagram $L_{12}^{(1+-)}$ describes non-diagonal transition $(A_{(Q_s)A_{(\bar{Q}\bar{s})}}) \rightarrow \{S_{(Q_s)A_{(\bar{Q}\bar{s})}}\}$, it is relatively small due to the partial cancellation of two contributions: $L_{12}^{(1+-)} = \frac{1}{2}g^2 (-L_{\psi\eta} + L_{\eta_c\phi})$.

In the general case the amplitude reads:

$$\begin{aligned} A_{(X \rightarrow \alpha)}^{(1+-)} &= g_{(X \rightarrow 1)} \frac{1}{\Delta^{(1+-)}} \left[d_1^{(1+-)} (1 - L_{22}^{(1+-)} d_2^{(1+-)}) + d_2^{(1+-)} L_{21}^{(1+-)} d_1^{(1+-)} \right] g_{(1 \rightarrow \alpha)} \\ &\quad + g_{(X \rightarrow 2)} \frac{1}{\Delta^{(1+-)}} \left[d_2^{(1+-)} (1 - L_{11}^{(1+-)} d_1^{(1+-)}) + d_1^{(1+-)} L_{12}^{(1+-)} d_2^{(1+-)} \right] g_{(2 \rightarrow \alpha)} \\ &= g_{(X \rightarrow 1)} \frac{1}{\nabla^{(1+-)}} \left[m_{1+-\{AS\}}^2 - s - L_{22}^{(1+-)} + L_{21}^{(1+-)} \right] g_{(1 \rightarrow \alpha)} \\ &\quad + g_{(X \rightarrow 2)} \frac{1}{\nabla^{(1+-)}} \left[m_{1+-\{AA\}}^2 - s - L_{11}^{(1+-)} + L_{12}^{(1+-)} \right] g_{(2 \rightarrow \alpha)}, \end{aligned} \quad (21)$$

where

$$\begin{aligned} \Delta^{(1+-)} &= (1 - L_{11}^{(1+-)} d_1^{(1+-)}) (1 - L_{22}^{(1+-)} d_2^{(1+-)}) - L_{12}^{(1+-)} d_2^{(1+-)} L_{21}^{(1+-)} d_1^{(1+-)}, \\ \nabla^{(1+-)} &= (m_{1+-\{AA\}}^2 - s - L_{11}^{(1+-)}) (m_{1+-\{AS\}}^2 - s - L_{22}^{(1+-)}) - L_{12}^{(1+-)} L_{21}^{(1+-)}. \end{aligned} \quad (22)$$

Bare masses $m_{1+-\{AA\}} \simeq (4380 - 4420)$ MeV and $m_{1+-\{AS\}} \simeq (4310 - 4350)$ MeV are given in eq. (9).

Zeros of the ∇ (eq.(22)) on the complex- s plane determine masses and widths of two resonances. Meson production densities for 1^{+-} - states are demonstrated in Fig. 6.

3.1.4 Two-pole amplitude for the 0^{++} - state

The wave functions for scalar states read:

$$\begin{aligned} \Psi_{(A_{(cs)A_{(\bar{c}\bar{s})}})}^{(0++)} &= \frac{1}{2\sqrt{3}} \left[\psi^{(0)}\phi^{(0)} - \psi^{(\uparrow)}\phi^{(\Downarrow)} - \psi^{(\Downarrow)}\phi^{(\uparrow)} + 3\eta_c\eta \right. \\ &\quad \left. - D_s^{*+(0)} D_s^{*-(0)} + D_s^{*+(\uparrow)} D_s^{*-(\Downarrow)} + D_s^{*+(\Downarrow)} D_s^{*-(\uparrow)} - 3D_s^+ D_s^- \right] \\ \Psi_{(S_{(cs)S_{(\bar{c}\bar{s})}})}^{(0++)} &= \frac{1}{2} \left[\psi^{(\uparrow)}\phi^{(\Downarrow)} + \psi^{(\Downarrow)}\phi^{(\uparrow)} - \psi^{(0)}\phi^{(0)} + \eta_c\eta \right. \\ &\quad \left. - D_s^{*+(0)} D_s^{*-(0)} + D_s^{*+(\uparrow)} D_s^{*-(\Downarrow)} + D_s^{*+(\Downarrow)} D_s^{*-(\uparrow)} + D_s^+ D_s^- \right]. \end{aligned} \quad (23)$$

For two 0^{++} levels one has three wave function convolutions:

$$\begin{aligned} \left\langle \Psi_{(A_{(cs)A_{(\bar{c}\bar{s})}})}^{(0++)} \middle| \Psi_{(A_{(cs)A_{(\bar{c}\bar{s})}})}^{(0++)} \right\rangle &= \\ \frac{1}{4} \langle \psi\phi | \psi\phi \rangle + \frac{3}{4} \langle \eta_c\eta | \eta_c\eta \rangle + \frac{1}{4} \langle D_s^{*+} D_s^{*-} | D_s^{*+} D_s^{*-} \rangle + \frac{3}{4} \langle D_s^+ D_s^- | D_s^+ D_s^- \rangle, \\ \left\langle \Psi_{(A_{(Q_s)A_{(\bar{Q}\bar{s})}})}^{(0++)} \middle| \Psi_{(S_{(Q_s)S_{(\bar{Q}\bar{s})}})}^{(0++)} \right\rangle &= \\ -\frac{\sqrt{3}}{4} \langle \psi\phi | \psi\phi \rangle + \frac{\sqrt{3}}{4} \langle \eta_c\eta | \eta_c\eta \rangle + \frac{\sqrt{3}}{4} \langle D_s^{*+} D_s^{*-} | D_s^{*+} D_s^{*-} \rangle - \frac{\sqrt{3}}{4} \langle D_s^+ D_s^- | D_s^+ D_s^- \rangle, \end{aligned} \quad (24)$$

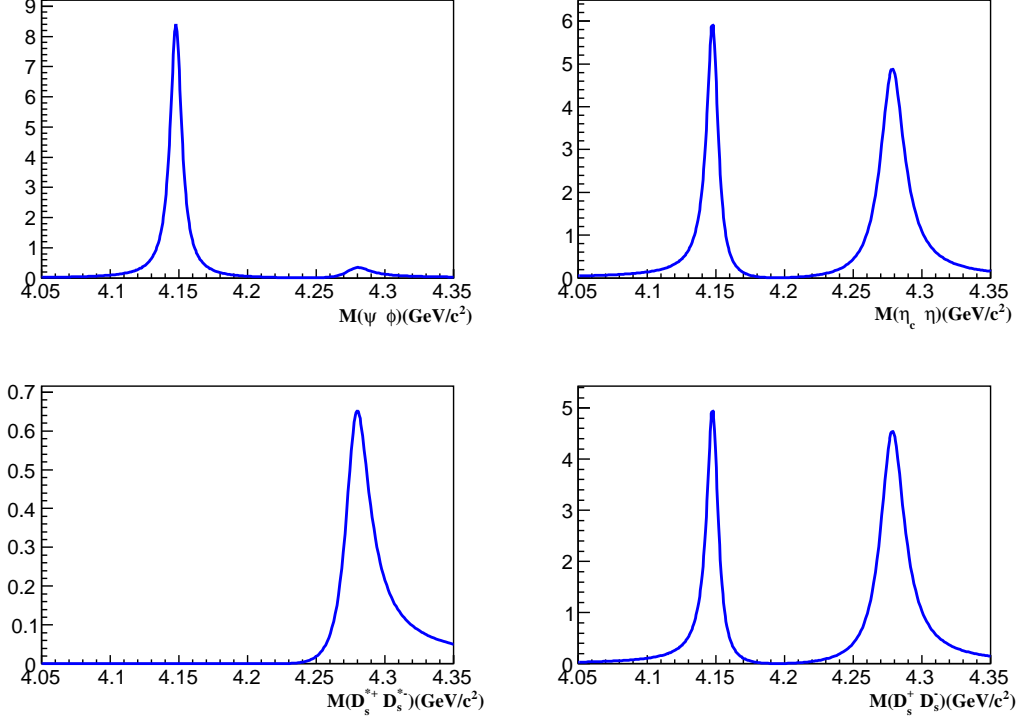


Figure 7: Production densities for the 0^{++} -states.

$$\begin{aligned} & \left\langle \Psi_{(S_{(Q_s)S_{(\bar{Q}\bar{s})})}^{(0^{++})}} \left| \Psi_{(S_{(Q_s)S_{(\bar{Q}\bar{s})})}^{(0^{++})} \right. \right\rangle = \\ & \frac{3}{4} \langle \psi\phi | \psi\phi \rangle + \frac{1}{4} \langle \eta_c\eta | \eta_c\eta \rangle + \frac{3}{4} \langle D_s^{*+} D_s^{*-} | D_s^{*+} D_s^{*-} \rangle + \frac{1}{4} \langle D_s^+ D_s^- | D_s^+ D_s^- \rangle, \end{aligned}$$

and three transition diagrams:

$$\begin{aligned} L_{11}^{(0^{++})} &= \frac{1}{4} g^2 L_{\psi\phi} + \frac{3}{4} g^2 L_{\eta_c\eta} + \frac{1}{4} g^2 L_{D_s^{*+} D_s^{*-}} + \frac{3}{4} g^2 L_{D_s^+ D_s^-}, \\ L_{12}^{(0^{++})} &= -\frac{\sqrt{3}}{4} g^2 L_{\psi\phi} + \frac{\sqrt{3}}{4} g^2 L_{\eta_c\eta} + \frac{\sqrt{3}}{4} g^2 L_{D_s^{*+} D_s^{*-}} - \frac{\sqrt{3}}{4} g^2 L_{D_s^+ D_s^-}, \\ L_{22}^{(0^{++})} &= \frac{3}{4} g^2 L_{\psi\phi} + \frac{1}{4} g^2 L_{\eta_c\eta} + \frac{3}{4} g^2 L_{D_s^{*+} D_s^{*-}} + \frac{1}{4} g^2 L_{D_s^+ D_s^-}. \end{aligned} \quad (25)$$

The amplitude reads:

$$\begin{aligned} A_{(X \rightarrow \alpha)}^{(0^{++})} &= g_{X_1} \frac{1}{\Delta^{(0^{++})}} \left[d_1^{(0^{++})} (1 - L_{22}^{(0^{++})} d_2^{(0^{++})}) + d_2^{(0^{++})} L_{21}^{(0^{++})} d_1^{(0^{++})} \right] g_{(1 \rightarrow \alpha)} \\ &+ g_{X_2} \frac{1}{\Delta^{(0^{++})}} \left[d_2^{(0^{++})} (1 - L_{11}^{(0^{++})} d_1^{(0^{++})}) + d_1^{(0^{++})} L_{12}^{(0^{++})} d_2^{(0^{++})} \right] g_{(2 \rightarrow \alpha)} \\ &= g_{X_1} \frac{1}{\nabla^{(0^{++})}} \left[m_{0^{++}(SS)}^2 - s - L_{22}^{(0^{++})} + L_{21}^{(0^{++})} \right] g_{(1 \rightarrow \alpha)} \\ &+ g_{X_2} \frac{1}{\nabla^{(0^{++})}} \left[m_{0^{++}(AA)}^2 - s - L_{11}^{(0^{++})} + L_{12}^{(0^{++})} \right] g_{(2 \rightarrow \alpha)}, \end{aligned} \quad (26)$$

where

$$\Delta^{(0^{++})} = (1 - L_{11}^{(0^{++})} d_1^{(0^{++})}) (1 - L_{22}^{(0^{++})} d_2^{(0^{++})}) - L_{12}^{(0^{++})} d_2^{(0^{++})} L_{21}^{(0^{++})} d_1^{(0^{++})},$$

$$\nabla^{(0^{++})} = \left(m_{0^{++}(AA)}^2 - s - L_{11}^{(0^{++})} \right) \left(m_{0^{++}(SS)}^2 - s - L_{22}^{(0^{++})} \right) - L_{12}^{(0^{++})} L_{21}^{(0^{++})}.$$

Production densities for the 1^{++} - state are shown in Fig. 7.

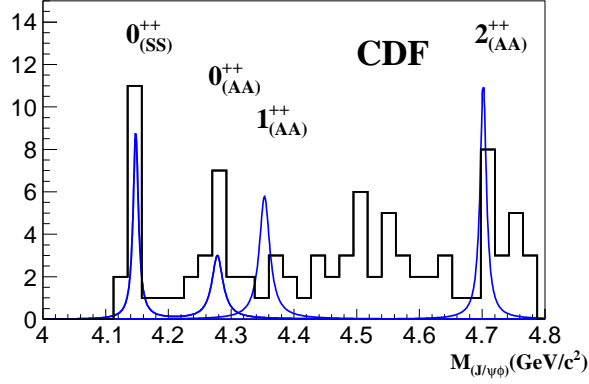


Figure 8: The CDF-spectrum [28] for $\phi J/\psi$ state in decay $B^\pm \rightarrow \phi(J/\psi)K^\pm$ and its comparison with the diquark-antidiquark model: $M_{0^{++}} \simeq 4140$ MeV, $M_{0^{++}} \simeq 4276$ MeV, $M_{1^{++}} \simeq 4278$ MeV, $M_{2^{++}} \simeq 4500$ MeV, the parameters are as follows: $m_S = 2072$ MeV, $m_A = 2137$ MeV, and $\Delta = 70$ MeV.

3.1.5 Meson-meson components and shifts of the resonance masses

The meson-meson component shifts pole positions. For different states they are as follows:

$$\begin{aligned} \delta m(0_{(AA)}^{++}) &= 173 \text{ MeV}, & \delta m(0_{(SS)}^{++}) &= 142 \text{ MeV}, \\ \delta m(1_{(AS)}^{++}) &= 153 \text{ MeV}, \\ \delta m(1_{(AA)}^{+-}) &= 111 \text{ MeV}, & \delta m(1_{(AS)}^{+-}) &= 68 \text{ MeV}, \\ \delta m(2_{(AA)}^{++}) &= 144 \text{ MeV}. \end{aligned} \quad (27)$$

The considered states are not molecular-like or deuteron-like systems that affected in hadronic values for the shifts of the resonance masses.

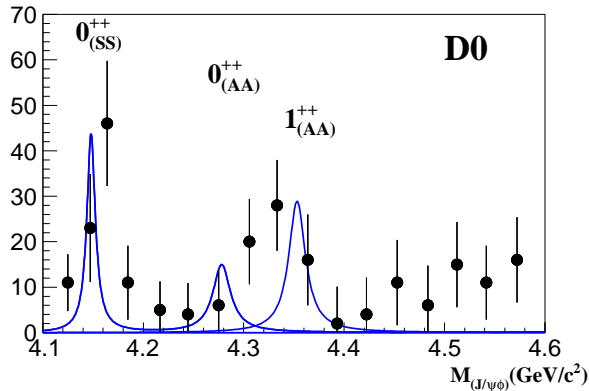


Figure 9: The D0-spectrum [30] for $(J/\psi\phi)$ state in decay $B^+ \rightarrow (\phi J/\psi)K^+$.

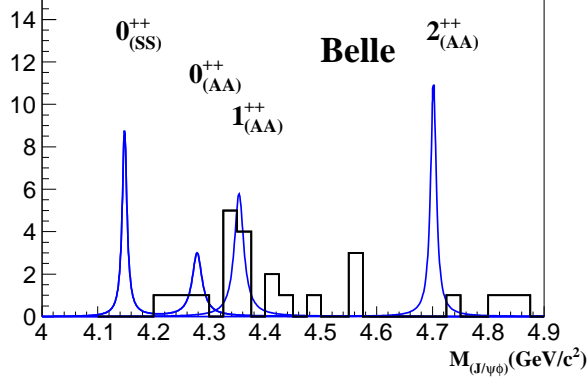


Figure 10: The Belle data [27] for reaction $\gamma\gamma \rightarrow \phi J/\psi$.

4 Data for $(\phi J/\psi)$ -spectra and diquark-antidiquark states

In Figs. 8 - 10 we demonstrate (J/ψ) - spectra measured by Belle [27], CDF [28] and D0 [30]. Using the classification of the diquark-antidiquark states suggested in Section 2.2.2 we compare calculated in Section 3 production densities with experimental data. The comparison allows to guess that eq. (9) leads to correct systematics of heavy exotic charmonia.

Fig. 10 shows that reaction of $\gamma^*\gamma^* \rightarrow X_{(s\bar{s})}^{(0^{++})}(4140) \rightarrow \phi J/\psi$ is relatively suppressed. Indeed, within vector dominance model, $\gamma^* \rightarrow J/\psi \rightarrow (c\bar{c})$ and $\gamma^* \rightarrow \phi \rightarrow (s\bar{s})$, we have for production ratio $R(\frac{SS(0^{++}) \rightarrow \phi\psi}{AS(1^{++}) \rightarrow \phi\psi}) \sim \frac{1}{4}$. This factor should be introduced additionally into production density curve in Fig. 10.

5 Exotic mesons with hidden strangeness as members of the nonet classification

Nonet classification of mesons ($\mathbf{1} + \mathbf{8}$) gives a standard and successful way for treating the $q\bar{q}$ states ($q = u, d, s$). It is reasonable to suggest that a similar classification works when constituents are diquarks. Then, considering the system of three diquarks, $((u\bar{c}), (d\bar{c}), (s\bar{c}))$ as an analog of the three-quark system (u, d, s) , we write six nonets for S-wave diquark-antidiquark systems:

		$(cq) \cdot (\bar{c}\bar{q})$ I=1	$(cq) \cdot (\bar{c}\bar{q})$ I=0	$(cs) \cdot (\bar{c}\bar{s})$ I=0	$(cq) \cdot (\bar{c}\bar{s})$ I = 1/2
2^{++}	$(A_{(cs)} \cdot A_{(\bar{c}\bar{s})})$	~ 4430	~ 4430	4630 ± 50	~ 4530
1^{+-}	$(A_{(cs)} \cdot A_{(\bar{c}\bar{s})})$	~ 4200	~ 4200	4400 ± 50	~ 4300
0^{++}	$(A_{(cs)} \cdot A_{(\bar{c}\bar{s})})$	~ 4080	~ 4080	4280 ± 20	~ 4180
1^{++}	$[A_{(cs)} \cdot S_{(\bar{c}\bar{s})}]$	~ 4180	~ 4180	4380 ± 20	~ 4280
1^{+-}	$\{A_{(cs)} \cdot S_{(\bar{c}\bar{s})}\}$	~ 4130	~ 4130	4330 ± 50	~ 4230
0^{++}	$(S_{(cs)} \cdot S_{(\bar{c}\bar{s})})$	~ 3930	~ 3930	4140 ± 20	~ 4040

Here we have used six diquark-antidiquark states with hidden strangeness, $(cs) \cdot (\bar{c}\bar{s})$, as a basis for the determination of masses of other nonet partners (masses are in MeV units). Weighting

of the strange quark is accepted to be $\Delta m_s = 100$ MeV, see discussion in Section 2, though the larger value, ~ 130 MeV, is possible.

Rich resonance structure in the exotic charmonium sector imply a principal concern in the study corresponding spectra: resonances in crossing channels or rescatterings in direct channels can affect determination of resonance characteristics, examples of such affections can be found in refs. [35, 36].

Search for resonance states in the $(cq) \cdot (\bar{c}\bar{q})$ sector was done in a series of studies, see refs. [33, 34, 37, 38, 39]. A set of candidates for non-strange exotic states is discussed in [1]. Nevertheless, reliable comparison of eq. (28) with data requires much more information.

6 Conclusion

We consider exotic mesons with hidden charm and strangeness in the mass region (4100 - 4800) MeV as two-component composite systems with (i) diquark-antidiquark component $(cs) \cdot (\bar{c}\bar{s})$, and (ii) meson-meson component $(c\bar{s}) \cdot (s\bar{c})$. The notion of diquarks is actively used in hadron physics both for mesons [19, 20, 21] and baryons [17, 18]. Following these ideas we construct a model in which the meson-meson component is taken into account in addition. Supposing that the recombination process $(cs) \cdot (\bar{c}\bar{s}) \rightarrow (c\bar{s}) \cdot (s\bar{c})$ dominates we calculate relative probabilities for decays into meson channels: $\psi\phi, \eta_c\eta, \eta_c\phi, \psi\eta, D_s^* \bar{D}_s^*, D_s^* \bar{D}_s, D_s \bar{D}_s^*, D_s \bar{D}_s$. Comparison with data [27, 28, 29, 30] is performed, Figs. 8, 9, 10. Predictions for new states are presented, and the nonet structure for $((Qq)(\bar{Q}\bar{q}), ((Qs)(\bar{Q}\bar{s})), ((Qq)(\bar{Q}\bar{s}))$ - states ($q = u, d$) is suggested in eq. (28).

Acknowledgment

We thank A.K. Likhoded and J. Nyiri for stimulating and useful discussions. The work was supported by grants RSGSS-4801.2012.2., RFBR-13-02-00425 and RSCF-14-22-00281 .

Appendix A Loop diagrams

We present loop diagrams for meson states calculated in terms of the dispersion relation technique, for details see for example ref. [4].

Appendix A.1 Loop diagram for one-pole and one-channel amplitude

Loop diagram above threshold, at $s > (M_a + M_b)^2$

The equation for one-pole and one-channel D-function reads:

$$D = d + D g^2 L d, \tag{A.1}$$

$$d = \frac{1}{m^2 - s}, \quad L = \int_{(M_a+M_b)^2}^{\infty} \frac{ds'}{\pi} \frac{\rho(s')}{s' - s - i0}.$$

Here m is a bare mass of this state, $g^2 L$ is loop diagram formed by hadrons, M_a, M_b are masses of the loop mesons. The phase space factor reads:

$$\rho_{ab}(s) = \frac{1}{16\pi s} \sqrt{[s - (M_a + M_b)^2][s - (M_a - M_b)^2]}. \quad (\text{A.2})$$

At $s < 4M^2$ we replace $\sqrt{s - 4M^2} \rightarrow i\sqrt{4M^2 - s}$, the point $s = 0$ is not singular for L .

The convergency of the integral for L_s can be organized either due to introducing a s -dependence of the vertex $g \rightarrow g(s)$ or by switching the subtraction procedure:

$$L_{(ab)}(s) = \int_{(M_a+M_b)^2}^{\infty} \frac{ds'}{\pi} \cdot \frac{\rho(s')}{s' - s - i0} \rightarrow \ell_0 + \int_{(M_a+M_b)^2}^{\infty} \frac{ds'}{\pi} \frac{s - (M_a + M_b)^2}{(s' - (M_a + M_b)^2)(s' - s - i0)} \rho(s'). \quad (\text{A.3})$$

In the (ab) -channel we write for positive s , $s > (M_a + M_b)^2$:

$$\begin{aligned} L_{(ab)}(s) &= \ell_0 + \frac{\lambda}{s} \\ &+ \frac{\sqrt{[s - (M_a + M_b)^2][s - (M_a - M_b)^2]}}{16\pi s} \left[\frac{1}{\pi} \ln \frac{\sqrt{s - (M_a - M_b)^2} - \sqrt{s - (M_a + M_b)^2}}{\sqrt{s - (M_a - M_b)^2} + \sqrt{s - (M_a + M_b)^2}} + i \right], \\ \lambda &= \frac{\sqrt{(M_a + M_b)^2(M_a - M_b)^2}}{16\pi^2} \ln \frac{\sqrt{(M_a + M_b)^2} + \sqrt{(M_a - M_b)^2}}{\sqrt{(M_a + M_b)^2} - \sqrt{(M_a - M_b)^2}}. \end{aligned} \quad (\text{A.4})$$

The point $s = (M_a + M_b)^2$ is singular. For $s < (M_a + M_b)^2$ we write $\sqrt{s - (M_a + M_b)^2} \rightarrow i\sqrt{(M_a + M_b)^2 - s}$, the points $s = (M_a - M_b)^2$ and $s = 0$ are not singular, the pole singularity at $s = 0$ is canceled due to choice of λ . The subtraction constant ℓ_0 is chosen to have zero value for loop diagram at threshold $L_{(ab)}(s)|_{s=(M_a+M_b)^2} = 0$, namely:

$$\ell_0 = \frac{-\lambda}{(M_a + M_b)^2}. \quad (\text{A.5})$$

Loop diagram below threshold, at $s < (M_a + M_b)^2$

At $(M_a - M_b)^2 < s < (M_a + M_b)^2$ the loop diagram reads:

$$\begin{aligned} L_{(ab)}(s) &= \ell_0 + \frac{\lambda}{s} \\ &+ i \frac{\sqrt{[-s + (M_a + M_b)^2][s - (M_a - M_b)^2]}}{16\pi s} \left[\frac{1}{\pi} \ln \frac{\sqrt{s - (M_a - M_b)^2} - i\sqrt{-s + (M_a + M_b)^2}}{\sqrt{s - (M_a - M_b)^2} + i\sqrt{-s + (M_a + M_b)^2}} + i \right] \\ &= \ell_0 + \frac{\lambda}{s} + i \frac{\sqrt{[-s + (M_a + M_b)^2][s - (M_a - M_b)^2]}}{16\pi s} \left[-\frac{2i}{\pi} \tan^{-1} \left(\frac{\sqrt{-s + (M_a + M_b)^2}}{\sqrt{s - (M_a - M_b)^2}} \right) + i \right]. \end{aligned} \quad (\text{A.6})$$

The last line demonstrates the absence of a singularity in $s = (M_a - M_b)^2$. Indeed, within top-down approaching to this point we have:

$$\begin{aligned} -\frac{2i}{\pi} \tan^{-1} \left(\frac{\sqrt{-s + (M_a + M_b)^2}}{\sqrt{s - (M_a - M_b)^2}} \right) + i &= -\frac{2i}{\pi} \left(\frac{\pi}{2} - \tan^{-1} \frac{\sqrt{s - (M_a - M_b)^2}}{\sqrt{-s + (M_a + M_b)^2}} \right) + i \\ &\simeq -\frac{2i}{\pi} \left(\frac{\pi}{2} - \frac{\sqrt{s - (M_a - M_b)^2}}{\sqrt{-s + (M_a + M_b)^2}} \right) + i \end{aligned}$$

with the corresponding cancellation of the singular terms in Eq. (A.6).

Appendix A.2 Multi-channel two-pole amplitude

Now we consider a realistic situation, multi-channel amplitude. For the one-pole case we write

$$\begin{aligned} A_{(X \rightarrow \alpha)} &= g_X \frac{d}{1 - \sum_{\alpha'} g_{\alpha'}^2 L_{\alpha'} d} g_{\alpha}. \quad (\text{A.7}) \\ L_{\alpha'} &= \int_{(M_a + M_b)^2}^{+\infty} \frac{ds'}{\pi} \frac{\rho_{\alpha'}(s')}{s' - s - i0}, \\ \alpha, \alpha' &= \psi\phi, \eta_c\eta, \psi\eta, \eta_c\phi, D_s \bar{D}_s, D_s^* \bar{D}_s, D_s \bar{D}_s^*, D_s^* \bar{D}_s^*. \end{aligned}$$

D -function for two-pole amplitude is equal to:

$$\begin{aligned} D_1 &= d_1 + D_1 L_{11} d_1 + D_2 L_{21} d_1, \\ D_2 &= d_2 + D_1 L_{12} d_2 + D_2 L_{22} d_2, \end{aligned} \quad (\text{A.8})$$

so the multi-channel two-pole amplitude reads:

$$\begin{aligned} A_{(X \rightarrow \alpha)} &= g_{(X \rightarrow 1)} D_1 g_{(1 \rightarrow \alpha)} + g_{(X \rightarrow 2)} D_2 g_{(2 \rightarrow \alpha)} = \quad (\text{A.9}) \\ g_{(X \rightarrow 1)} \frac{1}{\Delta} \left[d_1 (1 - g^2 L_{22} d_2) + d_2 L_{21} d_1 \right] g_{(1 \rightarrow \alpha)} &+ g_{(X \rightarrow 2)} \frac{1}{\Delta} \left[d_2 (1 - L_{11} d_1) + d_1 L_{12} d_2 \right] g_{(2 \rightarrow \alpha)}, \\ L_{if} &= \sum_{\alpha'} \int_{(M_a + M_b)^2}^{+\infty} \frac{ds'}{\pi} \frac{g_{i\alpha'} \rho_{\alpha'}(s') g_{f\alpha'}}{s' - s - i0}. \end{aligned}$$

Appendix B Spin wave functions of the $(cs \cdot \bar{c}\bar{s})$ systems and their decomposition into meson-meson space

For writing meson-meson loop diagrams we need to know the spin wave functions in meson-meson space - recombination of four-quark wave functions into two-meson ones is given below. To write meson spin convolutions, it is sufficient to know wave functions with one fixed component; we use $J_z = 0$ wave functions.

$A_{(cs)} \cdot A_{(\bar{c}\bar{s})}$ systems with $J^{PC} = 2^{++}$:

$$\begin{aligned}
\sqrt{6} \psi_{(A_{(cs)} A_{(\bar{c}\bar{s})})}^{(2,0)} &= \left(A_{(cs)}^{(\uparrow)} \cdot A_{(\bar{c}\bar{s})}^{(\Downarrow)} + 2 A_{(cs)}^{(0)} \cdot A_{(\bar{c}\bar{s})}^{(0)} + A_{(cs)}^{(\Downarrow)} \cdot A_{(\bar{c}\bar{s})}^{(\uparrow)} \right) \\
&= (c^\uparrow \bar{c}^\downarrow)(s^\uparrow \bar{s}^\downarrow) - (c^\uparrow \bar{s}^\downarrow)(s^\uparrow \bar{c}^\downarrow) + (c^\uparrow \bar{c}^\uparrow)(s^\downarrow \bar{s}^\downarrow) - (c^\uparrow \bar{s}^\downarrow)(s^\downarrow \bar{c}^\uparrow) \\
&\quad + (c^\uparrow \bar{c}^\downarrow)(s^\downarrow \bar{s}^\uparrow) - (c^\uparrow \bar{s}^\uparrow)(s^\downarrow \bar{c}^\downarrow) + (c^\downarrow \bar{c}^\uparrow)(s^\uparrow \bar{s}^\downarrow) - (c^\downarrow \bar{s}^\downarrow)(s^\uparrow \bar{c}^\uparrow) \\
&\quad + (c^\downarrow \bar{c}^\downarrow)(s^\uparrow \bar{s}^\uparrow) - (c^\downarrow \bar{s}^\uparrow)(s^\uparrow \bar{c}^\downarrow) + (c^\downarrow \bar{c}^\uparrow)(s^\downarrow \bar{s}^\uparrow) - (c^\downarrow \bar{s}^\uparrow)(s^\downarrow \bar{c}^\uparrow) \\
&= \left(2\psi^{(0)}\phi^{(0)} + \psi^{(\uparrow)}\phi^{(\Downarrow)} + \psi^{(\Downarrow)}\phi^{(\uparrow)} - 2D_s^{*(+)(0)} D_s^{*-(0)} - D_s^{*(+)(\uparrow)} D_s^{*-(\Downarrow)} - D_s^{*(+)(\Downarrow)} D_s^{*-(\uparrow)} \right).
\end{aligned} \tag{B.1}$$

$A_{(cs)} \cdot A_{(\bar{c}\bar{s})}$ systems with $J^{PC} = 1^{+-}$:

$$\begin{aligned}
\sqrt{2} \psi_{(A_{(cs)} A_{(\bar{c}\bar{s})})}^{(1,0)} &= \left(A_{(cs)}^{(\uparrow)} \cdot A_{(\bar{c}\bar{s})}^{(\Downarrow)} - A_{(cs)}^{(\Downarrow)} \cdot A_{(\bar{c}\bar{s})}^{(\uparrow)} \right) \\
&= (c^\uparrow \bar{c}^\downarrow)(s^\uparrow \bar{s}^\downarrow) - (c^\uparrow \bar{s}^\downarrow)(s^\uparrow \bar{c}^\downarrow) - (c^\downarrow \bar{c}^\uparrow)(s^\downarrow \bar{s}^\uparrow) + (c^\downarrow \bar{s}^\uparrow)(s^\downarrow \bar{c}^\uparrow) \\
&= \left(\psi^{(0)}\eta + \eta_c\phi^{(0)} - D_s^{*(+)(0)} D_s^- - D_s^+ D_s^{*-(0)} \right),
\end{aligned} \tag{B.2}$$

$A_{(cs)} \cdot A_{(\bar{c}\bar{s})}$ systems with $J^{PC} = 0^{++}$:

$$\begin{aligned}
\sqrt{3} \psi_{(A_{(cs)} A_{(\bar{c}\bar{s})})}^{(0,0)} &= \left(A_{(cs)}^{(\uparrow)} \cdot A_{(\bar{c}\bar{s})}^{(\Downarrow)} - A_{(cs)}^{(0)} \cdot A_{(\bar{c}\bar{s})}^{(0)} + A_{(cs)}^{(\Downarrow)} \cdot A_{(\bar{c}\bar{s})}^{(\uparrow)} \right) \\
&= (c^\uparrow \bar{c}^\downarrow)(s^\uparrow \bar{s}^\downarrow) - (c^\uparrow \bar{s}^\downarrow)(s^\uparrow \bar{c}^\downarrow) + (c^\downarrow \bar{c}^\uparrow)(s^\downarrow \bar{s}^\uparrow) - (c^\downarrow \bar{s}^\uparrow)(s^\downarrow \bar{c}^\uparrow) \\
&\quad - \frac{1}{2} \left[(c^\uparrow \bar{c}^\uparrow)(s^\downarrow \bar{s}^\downarrow) - (c^\uparrow \bar{s}^\downarrow)(s^\downarrow \bar{c}^\uparrow) + (c^\uparrow \bar{c}^\downarrow)(s^\downarrow \bar{s}^\uparrow) - (c^\uparrow \bar{s}^\uparrow)(s^\downarrow \bar{c}^\downarrow) \right. \\
&\quad \left. + (c^\downarrow \bar{c}^\uparrow)(s^\uparrow \bar{s}^\downarrow) - (c^\downarrow \bar{s}^\downarrow)(s^\uparrow \bar{c}^\uparrow) + (c^\downarrow \bar{c}^\downarrow)(s^\uparrow \bar{s}^\uparrow) - (c^\downarrow \bar{s}^\uparrow)(s^\uparrow \bar{c}^\downarrow) \right] \\
&= \frac{1}{2} \left(\psi^{(0)}\phi^{(0)} + 3\eta_c\eta - \psi^{(\uparrow)}\phi^{(\Downarrow)} - \psi^{(\Downarrow)}\phi^{(\uparrow)} \right. \\
&\quad \left. - D_s^{*(+)(0)} D_s^{*-(0)} - 3D_s^+ D_s^- + D_s^{*(+)(\uparrow)} D_s^{*-(\Downarrow)} + D_s^{*(+)(\Downarrow)} D_s^{*-(\uparrow)} \right).
\end{aligned} \tag{B.3}$$

$S_{(cs)} \cdot A_{(\bar{c}\bar{s})}$ and $A_{(cs)} \cdot S_{(\bar{c}\bar{s})}$ systems with $J^{PC} = 1^{++}$ and $J^{PC} = 1^{+-}$:

$$\begin{aligned}
2 \psi_{(S_{(cs)} A_{(\bar{c}\bar{s})})}^{(1,0)} &= 2 \left(S_{(cs)} \cdot A_{(\bar{c}\bar{s})}^{(0)} \right) \\
&= (c^\uparrow \bar{c}^\uparrow)(s^\downarrow \bar{s}^\downarrow) - (c^\uparrow \bar{s}^\downarrow)(s^\downarrow \bar{c}^\uparrow) + (c^\uparrow \bar{c}^\downarrow)(s^\downarrow \bar{s}^\uparrow) - (c^\uparrow \bar{s}^\uparrow)(s^\downarrow \bar{c}^\downarrow) \\
&\quad - (c^\downarrow \bar{c}^\uparrow)(s^\uparrow \bar{s}^\downarrow) - (c^\downarrow \bar{s}^\downarrow)(s^\uparrow \bar{c}^\uparrow) - (c^\downarrow \bar{c}^\downarrow)(s^\uparrow \bar{s}^\uparrow) + (c^\downarrow \bar{s}^\uparrow)(s^\uparrow \bar{c}^\downarrow) \\
&= \left(-\psi^{(0)}\eta + \eta_c\phi^{(0)} + \psi^{(\uparrow)}\phi^{(\Downarrow)} - \psi^{(\Downarrow)}\phi^{(\uparrow)} \right. \\
&\quad \left. + D_s^{*(+)(0)} D_s^- - D_s^+ D_s^{*-(0)} - D_s^{*(+)(\uparrow)} D_s^{*-(\Downarrow)} + D_s^{*(+)(\Downarrow)} D_s^{*-(\uparrow)} \right),
\end{aligned} \tag{B.4}$$

$$2 \psi_{(A_{(cs)} S_{(\bar{c}\bar{s})})}^{(1,0)} = 2 \left(A_{(cs)}^{(0)} \cdot S_{(\bar{c}\bar{s})} \right) \tag{B.5}$$

$$\begin{aligned}
&= (c^\uparrow \bar{c}^\uparrow)(s^\downarrow \bar{s}^\downarrow) - (c^\uparrow \bar{s}^\downarrow)(s^\downarrow \bar{c}^\uparrow) - (c^\uparrow \bar{c}^\downarrow)(s^\downarrow \bar{s}^\uparrow) + (c^\uparrow \bar{s}^\uparrow)(s^\downarrow \bar{c}^\downarrow) \\
&+ (c^\downarrow \bar{c}^\uparrow)(s^\uparrow \bar{s}^\downarrow) - (c^\downarrow \bar{s}^\downarrow)(s^\uparrow \bar{c}^\uparrow) - (c^\downarrow \bar{c}^\downarrow)(s^\uparrow \bar{s}^\uparrow) + (c^\downarrow \bar{s}^\uparrow)(s^\uparrow \bar{c}^\downarrow) \\
&= \left(\psi^{(0)} \eta - \eta_c \phi^{(0)} + \psi^{(\uparrow)} \phi^{(\downarrow)} - \psi^{(\downarrow)} \phi^{(\uparrow)} \right. \\
&\left. + D_s^{*+(0)} D_s^- - D_s^+ D_s^{*-(0)} + D_s^{*+(\uparrow)} D_s^{*-(\downarrow)} - D_s^{*+(\downarrow)} D_s^{*-(\uparrow)} \right).
\end{aligned}$$

The $S_{(cs)} \cdot S_{(\bar{c}\bar{s})}$ system with $J^{PC} = 0^{++}$:

$$\begin{aligned}
2\psi_{(A_{(cs)A_{(\bar{c}\bar{s})})}^{(0,0)}} &= 2 \left(S_{(cs)} \cdot S_{(\bar{c}\bar{s})} \right) \tag{B.6} \\
&= (c^\uparrow \bar{c}^\uparrow)(s^\downarrow \bar{s}^\downarrow) - (c^\uparrow \bar{s}^\downarrow)(s^\downarrow \bar{c}^\uparrow) - (c^\uparrow \bar{c}^\downarrow)(s^\downarrow \bar{s}^\uparrow) + (c^\uparrow \bar{s}^\uparrow)(s^\downarrow \bar{c}^\downarrow) \\
&\quad - (c^\downarrow \bar{c}^\uparrow)(s^\uparrow \bar{s}^\downarrow) + (c^\downarrow \bar{s}^\downarrow)(s^\uparrow \bar{c}^\uparrow) + (c^\downarrow \bar{c}^\downarrow)(s^\uparrow \bar{s}^\uparrow) - (c^\downarrow \bar{s}^\uparrow)(s^\uparrow \bar{c}^\downarrow) \\
&= \left(-\psi^{(0)} \phi^{(0)} + \eta_c \eta + \psi^{(\uparrow)} \phi^{(\downarrow)} + \psi^{(\downarrow)} \phi^{(\uparrow)} \right. \\
&\left. - D_s^{*+(0)} D_s^{*-(0)} + D_s^+ D_s^- + D_s^{*+(\uparrow)} D_s^{*-(\downarrow)} + D_s^{*+(\downarrow)} D_s^{*-(\uparrow)} \right).
\end{aligned}$$

References

- [1] PDG, J. Beringer et al., Phys. Rev. **D86**, 010001 (2012).
- [2] S. Godfrey, N. Isgur, Phys. Rev. **D32**, 189 (1985);
N. Isgur, *Quark confinement and the hadron spectrum*, Proc. 3rd Int.Conf., Newport News, June 1998.
- [3] R. Ricken, M. Koll, D. Merten, B.C. Metsch, H.R. Petry, Eur. Phys. J. **A9**, 73 (2000).
- [4] A.V. Anisovich, V.V. Anisovich, M.A. Matveev, V.A. Nikonov, J. Nyiri, A.V. Sarantsev *Mesons and Baryons*, World Scientific, Singapore (2008).
- [5] D.V. Bugg, Phys. Rev. **D87** (2013) 11, 118501.
- [6] E. Klempt and A. Zaitsev, Phys.Rept. **454**, 1 (2007).
- [7] V.V. Anisovich, Usp. Fiz. Nauk **174**, 49 (2004) [Physics-Uspekhi, **47**, 45 (2004)].
- [8] M. Gell-Mann, Phys. Lett. **8**, 214 (1964).
- [9] M. Ida and R. Kobayashi, Progr. Theor. Phys. **36**, 846 (1966).
- [10] D.B Lichtenberg and L.J. Tassie, Phys. Rev. **155**, 1601 (1967).
- [11] S. Ono, Progr. Theor. Phys. **48**, 964 (1972).
- [12] V.V. Anisovich, Pis'ma ZhETF **21**, 382 (1975) [JETP Lett. **21**, 174 (1975)];
V.V. Anisovich, P.E. Volkovitski, and V.I. Povzun, ZhETF **70**, 1613 (1976) [Sov. Phys. JETP **43**, 841 (1976)].
- [13] A. Schmidt and R. Blankenbeckler, Phys. Rev. **D16**, 1318 (1977)

- [14] M. Anselmino and E. Predazzi, eds., *Proceedings of the Workshop on Diquarks*, World Scientific, Singapore (1989).
- [15] K. Goeke, P.Kroll, and H.R. Petry, eds., *Proceedings of the Workshop on Quark Cluster Dynamics* (1992).
- [16] M. Anselmino and E. Predazzi, eds., *Proceedings of the Workshop on Diquarks II*, World Scientific, Singapore (1992).
- [17] A.V. Anisovich, V.V. Anisovich, M.A. Matveev, V.A. Nikonov, A.V. Sarantsev and T.O. Vulfs, *Int. J. Mod. Phys. A* **25**, 2965 (2010) [*Phys. Atom. Nucl.* **74**, 418 (2011)].
- [18] A.V. Anisovich, V.V. Anisovich, M.A. Matveev, V.A. Nikonov, J. Nyiri, A.V. Sarantsev *Three-particle physics and dispersion relation theory*, World Scientific, Singapore (2013).
- [19] L.Maiani, F.Piccinini, A.D.Polosa, V.Riquer, *Phys. Rev. D* **71**, 014028 (2005).
- [20] M.B. Voloshin, *Phys. Rev. D* **84**, 031502 (2011).
- [21] A. Ali, C. Hambrock, W.Wang, *Phys. Rev. D* **85**, 054011 (2012).
- [22] R.Jaffe, *Phys. Rev. D* **15**, 267,281 (1977).
- [23] G. Weinstein, N. Isgur, *Phys. Rev. D* **41**, 2236 (1990).
- [24] E. van Beveren, *Eur. Phys. J. C* **22**, 493 (2001).
- [25] V.V. Anisovich, L.G. Dakhno, M.A. Matveev, V.A. Nikonov and A.V. Sarantsev, *Yad. Fiz.* **70**, 392 (2007) [*Phys. Atom. Nucl.* **70**, 364 (2007)].
- [26] V.V. Anisovich, L.G. Dakhno, M.A. Matveev, V.A. Nikonov and A.V. Sarantsev, *Yad. Fiz.* **70**, 68 (2007) [*Phys. Atom. Nucl.* **70**, 63 (2007)].
- [27] Belle Collab.:
C.P. Shen et al., *Phys.Rev.Lett.* **104**, 112004 (2010); arXiv:0912.2383.
- [28] CDF-Collab.: T. Aaltonen et al., *Phys.Rev.Lett.* **102**, 242002 (2009); arXiv:0903.2229;
T. Aaltonen et al., arXiv:1101.6058[hep-ex] .
- [29] CMS-Collab.: arXiv:1309.6920[hep-ex] .
- [30] D0-Collab.: arXiv:1309.6580[hep-ex] .
- [31] A.V. Manohar, C.T. Sachrajda, *Phys. Rev. D* **66**, 010001-271 (2002).
- [32] LHCb-Collab.: arXiv:1202.5087[hep-ex] .
- [33] BABAR Collab.:
B. Aubert et al., *Phys. Rev. Lett.* **102**, 132001 (2009); arXiv:0809.0042[hep-ex];
B. Aubert et al., *Phys. Rev. Lett.* **101**, 082001 (2009); arXiv:0711.2047[hep-ex];
B. Aubert et al., arXiv:0607083[hep-ex];
J.P. Lees et al., arXiv:1111.5919[hep-ex];
B. Aubert et al., arXiv:0808.1543v2[hep-ex];
B. Aubert et al., *Phys. Rev. Lett.* **98**, 212001 (2007); arXiv:0506081[hep-ex];
B. Aubert et al., *Phys. Rev. D* **79**, 112001 (2009); arXiv:0811.0564[hep-ex].

- [34] Belle Collab.:
C.Z. Yuan et al., Phys. Rev. Lett. **99**, 182004 (2007); arXiv:0707.2541[hep-ex];
G. Pakhlova et al., Phys. Rev. D**77**, 011103R (2008); arXiv:0708.0082[hep-ex];
S.K. Choi et al., Phys. Rev. Lett. **100**, 142001 (2008); arXiv:0708.1790,[hep-ex];
P. Pakhlov et al., Phys. Rev. Lett. **100**, 202001 (2008); arXiv:0708.3812[hep-ex];
arXiv:0408124[hep-ex];
R. Mizuk et al., Phys. Rev. D**78**, 072004 (2008); arXiv:0806.4098 [hep-ex];
Phys. Rev. D**80**, 031104 (2009); arXiv:0905.2869[hep-ex].
- [35] V.V. Anisovich, D.V. Bugg, A.V. Sarantsev, B.S. Zou, Phys. Rev. D**50**, 1972 (1994).
- [36] V.V. Anisovich, D.V. Bugg, A.V. Sarantsev, B.S. Zou, Phys. Rev. D**51**, R4619-22 (1995).
- [37] LHCb Collab., R. Aaij et al., Phys.Rev.Lett. **112**, 222002 (2014);
Eur. Phys. J. **C72**, 1972 (2012);
arXiv:1112.5310[hep-ex].
- [38] CDF-Collab.: T. Aaltonen et al., Phys.Rev.Lett. **103**, 152001 (2009); arXiv:0906.5218[hep-ex].
- [39] CLEO Collab.:
T.E. Coan et al., Phys. Rev. Lett. **96**, 162003 (2006); arXiv:0602034[hep-ex];
Q. He et al., Phys. Rev. D**74**, 091104 (2006); arXiv:0611021[hep-ex].